

Cosmological parameters from complementary observations of the Universe

R. Durrer¹, B. Novosyadlyj²

¹ Department de Physique Théorique, Université de Genève, Quai Ernest Ansermet 24, CH-1211 Genève 4, Switzerland

² Astronomical Observatory of National University of L'viv, Kyryla and Mephodia str.8, 290005, L'viv, Ukraine

29 October 2018

ABSTRACT

We use observational data on the large scale structure (LSS) of the Universe measured over a wide range of scales from sub-galactic up to horizon scale and on the cosmic microwave background anisotropies to determine cosmological parameters within the class of adiabatic inflationary models. We show that a mixed dark matter model with cosmological constant (Λ MDM model) and parameters $\Omega_m = 0.37_{-0.15}^{+0.25}$, $\Omega_\Lambda = 0.69_{-0.20}^{+0.15}$, $\Omega_\nu = 0.03_{-0.03}^{+0.07}$, $N_\nu = 1$, $\Omega_b = 0.037_{-0.018}^{+0.033}$, $n_s = 1.02_{-0.10}^{+0.09}$, $h = 0.71_{-0.19}^{+0.22}$, $b_{cl} = 2.4_{-0.7}^{+0.7}$ (1σ confidence limits) matches observational data on LSS, the nucleosynthesis constraint, direct measurements of Hubble constant, the high redshift supernova type Ia results and the recent measurements of the location and amplitude of the first acoustic peak in the CMB anisotropy power spectrum. The best model is Λ dominated (65% of the total energy density) and has slightly positive curvature, $\Omega = 1.06$. The clustered matter consists in 8% massive neutrinos, 10% baryons and 82% cold dark matter (CDM). The upper 2σ limit on the neutrino content can be expressed in the form $\Omega_\nu h^2 / N_\nu^{0.64} \leq 0.042$ or, via the neutrino mass, $m_\nu \leq 4.0$ eV. The upper $1(2)\sigma$ limit for the contribution of a tensor mode to the COBE DMR data is $T/S < 1(1.5)$. Furthermore, it is shown that the LSS observations together with the Boomerang (+MAXIMA-1) data on the first acoustic peak rule out zero- Λ models at more than 2σ confidence limit.

Key words: Cosmology: large scale structure – microwave background anisotropies – cosmological models: power spectrum – cosmological parameters

1 INTRODUCTION

In the last decade of this century we have obtained important experimental results which play a crucial role for cosmology: the COsmic Background Explorer has discovered the large scale anisotropies of the cosmic microwave background radiation (Bennett et al. 1996); the High-Z Supernova Collaboration (Riess et al. 1998) and the Supernova Cosmology Project (Perlmutter et al. 1998) found that the universe is accelerating rather than decelerating; the Super-Kamiokande experiment (Fukuda et al. 1998) discovered neutrino oscillations which prove the existence of neutrinos with non-zero rest mass; balloon-borne measurements of the cosmic microwave background (CMB) temperature fluctuations by Boomerang (de Bernardis et al. 2000) and MAXIMA-1 (Hanany et al. 2000) have measured the height, position and width of the first acoustic peak which is in superb agreement with an adiabatic scenario of galaxy formation.

On the other hand the comparison of recent experimental data on the large scale structure of the Universe with

theoretical predictions of inflationary cosmology have shown since quite some time that the simplest cold dark matter (CDM) model is ruled out and we have to allow for a wider set of parameters to fit all observational data on the status and history of our Universe. These include spatial curvature (Ω_k), a cosmological constant (Ω_Λ), the Hubble parameter ($h \equiv H_0 / (100 \text{km/s/Mpc})$), the energy density of baryonic matter (Ω_b), cold dark matter (Ω_{cdm}), the number of species of massive neutrinos (N_ν) and their density (Ω_ν), the amplitude of the power spectra of primordial perturbations in scalar (A_s) and tensor (A_t) modes and the corresponding power-law indices (n_s and n_t), and the optical depth to early reionization (τ). Constraining this multidimensional parameter space, determining the true values of fundamental cosmological parameters, the nature and content of the matter which fills our Universe is an important and exciting problem of cosmology which has now become feasible due to the enormous progress in cosmological observations. About a dozen or more papers have been devoted to this problem in the last couple of years (see e.g. (Lineweaver & Barbosa 1998; Lineweaver 1998; Efstathiou & Bond 1999; Tegmark

1999; Bridle et al. 1999; Merchiorri et al. 2000; Novosyadlyj et al. 2000a; Tegmark & Zaldarriaga 2000a; Tegmark & Zaldarriaga 2000b; Lyth & Covi 2000; Novosyadlyj et al. 2000b; Lange et al. 2000; Balbi et al. 2000; Hu et al. 2000; Tegmark et al. 2000), some reviews are (Durrer & Straumann 1999; Sahni & Starobinsky 2000; Primack & Gross 2000; Primack 2000) and references therein).

However, in spite of this intensive investigations the problem is still not satisfactorily resolved. Some of the remaining issues are explained below.

First of all, we would like to have observations which 'measure' cosmological parameters in an as model independent way as possible. Clearly, most values of cosmological parameters obtained from observations of large scale structure, galaxy clustering and CMB anisotropies are strongly model dependent. If the 'correct' model of structure formation is not within the family investigated, we may not notice it, especially if the error bars are relatively large. This leads us to the next problem. Even if cosmological observation have improved drastically, we still need more accurate data with better defined statistical properties (e.g we need to know the correlation of different measurements). The new CMB anisotropy data are already of this quality but the galaxy and cluster data are still relatively far from it.

A next important point is the correspondence between theoretical predictions and observational characteristics used in the analysis. We have to find a fast but accurate way to compute the theoretical values, especially when exploring high dimensional parameter spaces. All parameters must be fitted simultaneously which renders the problem computationally complicated and very time consuming. Due to this difficulty, many authors search some subset of parameters setting the others to some fixed 'reasonable' priors, thereby investigating a sub-class of cosmological models. As different authors also use different subsets of observational data, the resulting cosmological parameters still vary in a relatively wide range.

Another problem are the degeneracies in parameter space which appear especially in the case when only CMB anisotropy data are used (Efstathiou & Bond 1999). It can be reduced substantially or even removed completely if galaxy clustering data, corresponding to different scales and redshifts, are combined with CMB measurements. This idea has already been employed on several occasions and is known under the name 'cosmic concordance' (for a recent review see Tegmark et al. 2000c)).

The goal of this paper is to determine cosmological parameters of the sub-class of models without tensor mode and no early reionization on the basis of LSS data related to different scales and different redshifts. In Novosyadlyj et al. (2000a) we have used the same approach to test flat models; we have shown that AMDM models are preferred in this class of models. There we have also shown that pure CDM models with $h \geq 0.5$, scale invariant primordial power spectrum, vanishing cosmological constant and spatial curvature are ruled out at very high confidence level, more than 99.99%. The corresponding class of mixed dark matter (MDM) models are ruled out at about 95% C.L. It was noted (Novosyadlyj et al. 2000b) that the galaxy clustering data set determines the amplitude of scalar fluctuations approximately at the same level as the COBE four-year

data. This indicates that a possible tensor component in the COBE data cannot be very substantial.

In this paper we test AMDM models with non-zero curvature. Furthermore, we use the data on the location and amplitude of the first acoustic peak determined from the most accurate recent measurements of the CMB power spectrum. The data on the amplitude of the 2-nd and 3-d peaks is used as additional test for model preferred by large scale structure, COBE and 1-st peak data. We investigate the (in-)consistency of our data set with the 2-nd and 3-d peaks. We also use the SNIa constraint for comparison.

The outline of the paper is as follows: in Sect. 2 we describe the experimental data set which is used here. The calculations of theoretical predictions and the method employed to determine cosmological parameters are described in Sect. 3. In Sect. 4 we discuss our results and compare them with other investigations. Our conclusions are presented in Sect. 5.

2 THE EXPERIMENTAL DATA SET

Our approach is based on the quantitative comparison of the theoretical predictions for the characteristics of the large scale structure of the Universe with corresponding observational ones. Theoretical predictions are calculated on the base of initial power spectrum of density perturbations of which shape strongly depends on all parameters supposed here for determination. So, model independent observational constraints on the inclination and amplitude of the power spectrum at different scales will be used in this search.

2.1 CMB data

We use the COBE 4-year data on CMB temperature anisotropies (Bennett et al. 1996) to normalize the density fluctuation power spectra according to Liddle et al. (1996) and Bunn & White (1997). Therefore, each model will match the COBE data by construction.

We believe that using all available experimental data on $\Delta T/T$ at angular scales smaller than the COBE measurement is not an optimal way to search best-fit cosmological parameters due to their large dispersion (see for examples Fig.10.1 of Durrer & Straumann 1999, Fig.2 of Novosyadlyj et al. 2000a or Fig.1 of Tegmark et al. 2000) which together with the large number of experimental points, ~ 70 stipulating a high degrees of freedom, result in wide ranges for the confidence limits on cosmological parameters. The Boomerang (de Bernardis et al. 2000) and MAXIMA-1 (Hanany et al. 2000) experiments represent a new generation of CMB measurements. They have produced a CMB map of about $\sim 100\text{deg}^2$ with a resolution better than half a degree and a $S/N \sim 2$, which allows to determine the location and amplitude of the first acoustic peak with high accuracy. The position of the first and amplitudes of the first, second and third acoustic peaks in the angular power spectrum of the CMB temperature fluctuations together with the COBE data are the main measured characteristics of the CMB power spectrum. They contain information about amplitude and tilt of the primordial power spectrum of density fluctuations at largest scales, from few tens of Mpc up to the current horizon scale of several thousand Mpc. They

are mainly sensitive to the parameters Ω_k , $\Omega_m h^2$, Ω_Λ , $\Omega_b h^2$, n_s and to the normalization of the initial power spectrum of density fluctuations.

For example, the Boomerang data indicate that the first peak is located at the Legendre multipole $\tilde{\ell}_p = 197 \pm 6$ and has an amplitude of $\tilde{A}_p = 69 \pm 8 \mu\text{K}$ (this 1σ error includes statistical and calibration errors). Here and in the following a tilde denotes observed quantities. We use these results in our search procedure. The MAXIMA-1 data ($\tilde{\ell}_p \approx 220$, $\tilde{A}_p = 78 \pm 6 \mu\text{K}$) marginally match Boomerang data and we will show that using them in combination with Boomerang data does not change the results significantly. The positions of 2-nd and 3-d peaks are not well determined and we will not use them in the main search procedure but we use their amplitudes as determined by (Hu et al. 2000) for comparison with the predictions of our best-fit model.

2.2 Rich cluster data

The important constraints on the form and amplitude of the matter power spectrum in the range from $10h^{-1}\text{Mpc}$ up to scales approaching $1000h^{-1}\text{Mpc}$ can be obtained from the study of clusters of galaxies, their space distribution, mass and X-ray temperature functions.

The power spectrum reconstructed from the observed space distribution of clusters has been determined many times for different samples from Abell, ACO and APM catalogs (see Einasto et al. 1997, Retzlaff et al. 1998, Tadros et al. 1998, Miller and Batuski 2000 and references therein). The remarkable feature of the determinations by different groups is similar slopes of cluster power spectra on scales $0.02h\text{Mpc}^{-1} \leq k \leq 0.1h\text{Mpc}^{-1}$, $n \sim -1.5$ (see above mentioned references). Here, we use the power spectrum of Abell-ACO clusters $\tilde{P}_{A+ACO}(k_j)$ (Retzlaff et al. 1998) as observational input. It is measured in the range $0.03h/\text{Mpc} \leq k \leq 0.2h/\text{Mpc}$ where effects of nonlinear evolution are negligible and it has well analyzed sources of uncertainties. The cluster power spectrum is biased with respect to the dark matter distribution. We assume that the bias is linear and scale independent. This is reasonable in the range of scales considered as predicted from local bias models (Fry & Gaztañaga 1993) and indicated by numerical simulations (Benson et al. 2000). In our previous paper (Novosyadlyj et al. 2000a) we have shown that not all the 13 points given in Retzlaff et al. (1998) are independent measurements and the effective number of degrees of freedom is 3. But to make best use of the observational information we use all 13 points of the power spectrum to determine cosmological parameters and assign $n_F = 3$ for the number of degrees of freedom in the marginalization procedure.

A constraint for the amplitude of the fluctuation power spectrum on cluster scale can be derived from the cluster mass and the X-ray temperature functions. It is usually formulated as constraint for the density fluctuation in a top-hat sphere of $8h^{-1}\text{Mpc}$ radius, σ_8 , which can be calculated for a given initial power spectrum $P(k)$ by

$$\sigma_8^2 = \frac{1}{2\pi^2} \int_0^\infty k^2 P(k) W^2(8\text{Mpc } k/h) dk, \quad (1)$$

where $W(x) = 3(\sin x - x \cos x)/x^3$ is the Fourier transform of a top-hat window function. Recent optical determinations

of the mass function of nearby galaxy clusters (Girardi et al. 1998) give

$$\tilde{\sigma}_8 \Omega_m^{\alpha_1} = 0.60 \pm 0.04 \quad (2)$$

where $\alpha_1 = 0.46 - 0.09\Omega_m$ for flat low-density models and $\alpha_1 = 0.48 - 0.17\Omega_m$ for open models (at the 90% C.L.). Several groups have found similar results using different methods and different data sets (for a comprehensive list of references see Borgani et al. (1999)). This constraint on σ_8 is exponentially sensitive and thus allows only very small error bars. If the theory is correct this is of course a great advantage. However, if our understanding of cluster formation is not entirely correct, this will lead to discrepancies with other experimental constraints.

From the observed evolution of the cluster X-ray temperature distribution function between $z = 0.05$ and $z = 0.32$ we use the following constraint derived by Viana & Lidde (1999)

$$\tilde{\sigma}_8 \Omega_m^{\alpha_2} = 0.56 \pm 0.19 \Omega_m^{0.1 \lg \Omega_m + \alpha_2}, \quad \alpha_2 = 0.34$$

for open models and

$$\tilde{\sigma}_8 \Omega_m^{\alpha_2} = 0.56 \pm 0.19 \Omega_m^{0.2 \lg \Omega_m + \alpha_2}, \quad \alpha_2 = 0.47$$

for flat models (both with 95% confidence limits).

From the existence of three very massive clusters of galaxies observed so far at $z > 0.5$ an additional constraint has been established by (Bahcall & Fan 1998)

$$\tilde{\sigma}_8 \Omega_m^{\alpha_3} = 0.8 \pm 0.1, \quad (3)$$

where $\alpha_3 = 0.24$ for open models and $\alpha_3 = 0.29$ for flat models.

Note that all these constraints are given by slightly different formulas for either $\Omega_\Lambda = 0$ or $\Omega_\Lambda + \Omega_m = 1$. However, we are going to use them for arbitrary values of Ω_Λ and Ω_m . Since our best fit models are relatively close to the flat model, we mainly use the formula for the flat case. We have checked that our results are insensitive to this choice.

2.3 Peculiar velocity data

Since our approach is based on the initial power spectrum of density fluctuations it seems most favorable to use the power spectrum reconstructed from the observed space distribution of galaxies. But the galaxy power spectra obtained from the two-dimensional APM survey (e.g. (Maddox et al. 1996; Tadros & Estathiou 1996), and references therein), the CfA redshift survey (Vogeley et al. 1992; Park et al. 1994), the IRAS survey (Saunders et al. 1992; Saunders et al. 2000) and the Las Campanas Redshift Survey (da Costa et al. 1994; Landy et al. 1996) differ significantly in both, the amplitude and the position of the maximum. Moreover, nonlinear effects on small scales must be taken into account in their analysis. On the other hand, these power spectra contain large number of experimental points which are not independent and a decorrelation procedure for these power spectra must be employed. For these reasons and also in order to test the consistency between different data set, we do not include galaxy power spectra for the determination of parameters in this work. It will be interesting to compare our best fit parameters with those obtained in analyzes including galaxy power spectra.

Another constraint on the amplitude of the linear power

spectrum of density fluctuations in our vicinity comes from the study of bulk flows of galaxies in spheres of large enough radii around our position. Since these data may be influenced by the local super-cluster (cosmic variance), we will use only the value of the bulk motion - the mean peculiar velocity of galaxies in a sphere of radius $50h^{-1}\text{Mpc}$ given by (Kolatt & Dekel 1997),

$$\tilde{V}_{50} = (375 \pm 85)\text{km/s.} \quad (4)$$

With its generous error bars, this value is in a good agreement with other measurements of bulk motion at the scale $40 - 60h^{-1}\text{Mpc}$ (Bertschinger et al. 1990; Courteau et al. 1993; Dekel 1994) (see also the review by Dekel 1999).

2.4 Ly- α constraints

An important constraint on the linear matter power spectrum on small scales ($k \sim (2 - 40)h/\text{Mpc}$) comes from the Ly- α forest, the Ly- α absorption lines seen in quasar spectra (see Gnedin (1998), Croft et al. (1998) and references therein). Assuming that the Ly- α forest is formed by discrete clouds with a physical size close to the Jeans scale in the reionized inter-galactic medium at $z \sim 2 - 4$, Gnedin (1998) has derived a constraint on the value of the r.m.s. linear density fluctuations

$$1.6 < \tilde{\sigma}_F(z = 3) < 2.6 \quad (95\%\text{C.L.}) \\ \text{at } k_F \approx 34\Omega_m^{1/2}h/\text{Mpc}.$$

Taking into account the new data on quasar absorption lines, the effective equation of state and the temperature of the inter-galactic medium at high redshift were re-estimated recently (Ricotti et al. 1999). As a result the value of Jeans scale at $z = 3$ has moved to $k_F \approx 38\Omega_m^{1/2}h/\text{Mpc}$ (Gnedin 2000). Here, we adopt this new value.

The procedure to recover the linear power spectrum from the Ly- α forest has been elaborated by Croft et al. (1998). Analyzing the absorption lines in a sample of 19 QSO spectra, they have obtained the following constraint on the amplitude and slope of the linear power spectrum at $z = 2.5$ and $k_p = 1.5\Omega_m^{1/2}h/\text{Mpc}$,

$$\tilde{\Delta}_\rho^2(k_p) \equiv k_p^3 P(k_p)/2\pi^2 = 0.57 \pm 0.26, \quad (6)$$

$$\tilde{n}_p \equiv \frac{\Delta \log P(k)}{\Delta \log k} \Big|_{k_p} = -2.25 \pm 0.18, \quad (7)$$

at (1σ C.L.). The like constraints on the amplitude and slope of the linear power spectrum was obtained by (McDonald et al. 2000) from the analysis of absorption lines in a sample of 8 QSO. We will analyze these constraints in the context of our task and compare them with previous two. But in the main search procedure we will use the constraints given by Croft et al. (1998) as based on the more extensive sample of quasars.

2.5 Other experimental constraints

In addition to the CMB & LSS measurements described above we also use some results of global observations which are independent of the LSS model. For the value of the Hubble constant we set

$$\tilde{h} = 0.65 \pm 0.10, \quad (8)$$

which is a compromise between measurements made by two groups, (Tammann & Federspiel 1997) and (Madore et al. 1999). We also employ a nucleosynthesis constraint on the baryon density deduced from the determination of the primeval deuterium abundance

$$\widetilde{\Omega_b h^2} = 0.019 \pm 0.0024 \quad (95\%\text{C.L.}) \quad (9)$$

given by Burles et al. (1999). The new, more precise determination (Burles et al. 2000) confirms this value.

Furthermore, we include the distance measurements of super novae of type Ia (SNIa) which constrain the cosmic expansion history (Riess et al. 1998; Perlmutter et al. 1998; Perlmutter et al. 1999). In a universe with cosmological constant this gives an important constraint on a combination of the values of the curvature, the cosmological constant and the matter content of the Universe. We use the following constraint in our parameter search (Perlmutter et al. 1999)

$$[\Omega_m - \widetilde{0.75\Omega_\Lambda}] = -0.25 \pm 0.125. \quad (10)$$

3 THE METHOD AND SOME TESTS

One of the main ingredients for the solution for our search problem is a reasonably fast and accurate determination of the linear transfer function for dark matter clustering which depends on the cosmological parameters. We use accurate analytical approximations of the MDM transfer function $T(k; z)$ depending on the parameters Ω_m , Ω_b , Ω_ν , N_ν and h by Eisenstein & Hu (1999). According to this work, the linear power spectrum of matter density fluctuations is given by

$$P(k; z) = A_s k^{n_s} T^2(k; z) D_1^2(z)/D_1^2(0), \quad (11)$$

where A_s is the normalization constant for scalar perturbations and $D_1(z)$ is the linear growth factor, which can be approximated by (Carroll et al. 1992)

$$D_1(z) = \frac{5}{2} \frac{\Omega_m(z)}{1+z} \left[\frac{1}{70} + \frac{209\Omega_m(z) - \Omega_m^2(z)}{140} + \Omega_m^{4/7}(z) \right]^{-1},$$

where

$$\Omega_m(z) = \Omega_m(1+z)^3 / (\Omega_m(1+z)^3 + \Omega_\Lambda + \Omega_k(1+z)^2).$$

We normalize the spectra to the 4-year COBE data which determine the amplitude of density perturbation at horizon scale, δ_h (Liddle et al. 1996; Bunn and White 1997). The normalization constant A_s is then given by

$$A_s = 2\pi^2 \delta_h^2 (3000\text{Mpc}/h)^{3+n_s}. \quad (12)$$

The Abell-ACO power spectrum is related to the matter power spectrum at $z = 0$, $P(k; 0)$, by the cluster biasing parameter b_{cl} . As argued above, we assume scale-independent, linear bias

$$P_{A+ACO}(k) = b_{cl}^2 P(k; 0). \quad (13)$$

For a given set of parameters Ω_m , Ω_Λ , Ω_b , Ω_ν , N_ν , n_s , h , and b_{cl} the theoretical values of $P_{A+ACO}(k_j)$ can now be obtained for the values k_j (Table 1 of (Novosyadlyj et al. 2000a)). We denote them by y_j ($j = 1, \dots, 13$).

The dependence of the position and amplitude of the first acoustic peak in the CMB power spectrum on cosmological parameters has been investigated using CMBfast (Seljak & Zaldarriaga 1996). As expected, and as we have shown in

our previous paper (Novosyadlyj et al. 2000a), the results are, within reasonable accuracy, independent on the fraction of hot dark matter, $f_\nu = \Omega_\nu/\Omega_m$, up to $f_\nu \approx 0.6$.

For the remaining parameters, n_s , h , Ω_b , Ω_{cdm} and Ω_Λ , we determine the resulting values ℓ_p and A_p using the analytical approximation given by Efstathiou & Bond (1999). We extend the approximation to models with non-zero curvature ($\Omega_k \equiv 1 - \Omega_m - \Omega_\Lambda \neq 0$) by adding a coefficient for the amplitude and the peak location, which is determined numerically. The analytical approximation for the position of the first acoustic peak used here is

$$\ell_p = 0.746\pi\sqrt{3(1+z_r)}\frac{R(\omega_m, \omega_k, y)}{I_s(\omega_m, \omega_b)}, \quad (14)$$

where $\omega_* \equiv \Omega_* h^2$, and $R = \omega_m^{1/2} \frac{\sinh(\omega_k^{1/2} y)}{\omega_k^{1/2}}$, $\omega_m^{1/2} y$, $\omega_m^{1/2} \frac{\sin(\omega_k^{1/2} y)}{|\omega_k|^{1/2}}$ for open, flat and closed models respectively. Here $y(\omega_m, \omega_k, \omega_\Lambda)$ is given by formula (8b) and $I_s(\omega_m, \omega_b)$ by formulae (17-19) of Efstathiou & Bond (1999). The accuracy of this analytical approximation is better than 1%.

The approximation for the amplitude of first acoustic peak is as follows:

$$A_p = \left(\frac{\ell_p(\ell_p+1)}{2\pi} C_2 \frac{\Gamma(l_p + \frac{n_s+1}{2}) \Gamma(\frac{9-n_s}{2})}{\Gamma(l_p + \frac{5-n_s}{2}) \Gamma(\frac{3+n_s}{2})} + 0.838A(\omega_b, \omega_{cdm}, n_s) \right)^{1/2}, \quad (15)$$

where $\ln A(\omega_b, \omega_{cdm}, n_s) = 4.5(n_s - 1) + a_1 + a_2\omega_{cdm}^2 + a_3\omega_{cdm} + a_4\omega_b^2 + a_5\omega_b + a_6\omega_b\omega_{cdm} + a_7\omega_k$, with $a_1 = 2.376$, $a_2 = 3.681$, $a_3 = -5.408$, $a_4 = -54.262$, $a_5 = 18.909$, $a_6 = 15.384$, $a_7 = 4.2$ and C_2 is the quadrupole anisotropy approximated by

$$C_2 = A_s \frac{\pi}{16} \left(\frac{H_0}{c} \right)^{n_s+3} \frac{\Gamma(3-n_s)}{\Gamma^2(\frac{4-n_s}{2})} \frac{\Gamma(2+\frac{n_s+1}{2})}{\Gamma(2+\frac{5-n_s}{2})}. \quad (16)$$

The values $a_1 - a_6$ are the best-fit coefficients determined from a grid of models computed with CMBfast (Efstathiou & Bond 1999). We have added the coefficient a_7 in order to account for curvature. The accuracy of A_p in the parameter ranges which we consider is better than 5%. We denote ℓ_p and A_p by y_{14} and y_{15} respectively.

The theoretical values of the other experimental constraints are obtained as follows: the density fluctuation σ_8 is calculated according to Eq. (1) with $P(k; z)$ taken from Eq. (11). We set $y_{16} = \sigma_8 \Omega_m^{\alpha_1}$, $y_{17} = \sigma_8 \Omega_m^{\alpha_2}$ and $y_{18} = \sigma_8 \Omega_m^{\alpha_3}$ with corresponding values of α_i ($i=1, 2, 3$) for vanishing and non-zero curvature (see previous section).

The r.m.s. peculiar velocity of galaxies in a sphere of radius $R = 50h^{-1}\text{Mpc}$ is given by

$$V_{50}^2 = \frac{1}{2\pi^2} \int_0^\infty k^2 P^{(v)}(k) e^{-k^2 R_f^2} W^2(50\text{Mpc } k/h) dk, \quad (17)$$

where $P^{(v)}(k)$ is power spectrum for the velocity field of the density-weighted matter (Eisenstein & Hu 1999), $W(50\text{Mpc } k/h)$ is the top-hat window function. A previous smoothing of the raw data with a Gaussian filter of radius $R_f = 12h^{-1}\text{Mpc}$ is employed, similar to the procedure which has led to the observational value. For the scales of interest $P^{(v)}(k) \approx (\Omega^{0.6} H_0)^2 P(k; 0)/k^2$. We denote the r.m.s. peculiar velocity by y_{19} .

The value by Gnedin (1998) from the formation of Ly- α clouds constrains the r.m.s. linear density perturbation at redshift $z = 3$ and wave number $k_F = 38\Omega_m^{1/2}h/\text{Mpc}$. In terms of the power spectrum, σ_F is given by

$$\sigma_F^2(z) = \frac{1}{2\pi^2} \int_0^\infty k^2 P(k; z) e^{(-k/k_F)^2} dk. \quad (18)$$

It will be denoted by y_{20} . The corresponding value of the constraint by Croft et al. (1998) is

$$\Delta_p^2(k_p, z) \equiv k_p^3 P(k_p, z)/2\pi^2, \quad (19)$$

at $z = 2.5$ with $k_p = 0.008H(z)/(1+z)(\text{km/s})^{-1}$, will be denoted by y_{21} ;

$H(z) = H_0 [\Omega_m(1+z)^3 + \Omega_k(1+z)^2 + \Omega_\Lambda]^{1/2}$ is the Hubble parameter at redshift z . The slope of the power spectrum at this scale and redshift,

$$n_p(z) \equiv \frac{\Delta \log P(k, z)}{\Delta \log k}, \quad (20)$$

is denoted by y_{22} .

For all tests except Gnedin's Ly- α clouds, we use the density weighted transfer function $T_{cb\nu}(k, z)$ from (Eisenstein & Hu 1999). For Gnedin's σ_F we use $T_{cb}(k, z)$ according to the prescription of Gnedin (1998). It must be noted that even in the model with maximal Ω_ν (~ 0.2) the difference between $T_{cb}(k, z)$ and $T_{cb\nu}(k, z)$ is less than 12% for $k \leq k_p$. Early reionization changes somewhat the evolution of density perturbation in the baryon component on small scales. This effect is not taken into account by the analytical approximation used here (Eisenstein & Hu 1999). Therefore, we restrict ourselves to models without early reionization. We calculate the Ly- α tests according to the prescription given in Sect. 5.4 of (Eisenstein & Hu 1999).

Finally, the values of $\Omega_b h^2$, h and $\Omega_m - 0.75\Omega_\Lambda$ are denoted by y_{23} , y_{24} and y_{25} respectively.

The squared differences between the theoretical and observational values divided by the observational error are given by χ^2 ,

$$\chi^2 = \sum_{j=1}^{23} \left(\frac{\tilde{y}_j - y_j}{\Delta \tilde{y}_j} \right)^2. \quad (21)$$

Here \tilde{y}_j and $\Delta \tilde{y}_j$ are the experimental data and their dispersion, respectively. The set of parameters Ω_m , Ω_Λ , Ω_ν , Ω_b , h , n_s and b_{cl} are then determined by minimizing χ^2 using the Levenberg-Marquardt method (Press et al. 1992). The derivatives of the predicted values with respect to the search parameters which are required by this method are obtained numerically using a relative step size of 10^{-5} with respect to the given parameter.

In order to test our method for stability, we have constructed a mock sample of observational data. We start with a set of cosmological parameters and determine the "observational" data for them which would be measured in case of faultless measurements with 1σ errors comparable to the observational errors. We then insert random sets of starting parameters into the search program and try to recover the model which corresponds to the mock data. The method is stable if we can recover our input cosmological model (for more details of this test procedure see Novosyadlyj et al. (2000a). The code finds all the previously known parameters with high accuracy. Even starting very far away from the

true values, our method reveals as very stable and finds the 'true' model whenever possible. This means that the code finds the global minimum of χ^2 independent of the initial values for the parameters. This also hints that our data set is sufficiently divers to be free of degeneracies (which plague parameter searches working with CMB data only).

4 RESULTS AND DISCUSSION

4.1 Calculations

The determination of the parameters ${}^*\Omega_m, \Omega_\Lambda, \Omega_\nu, N_\nu, \Omega_b, h, n_s$ and b_{cl} by the Levenberg-Marquardt χ^2 minimization method (Press et al. 1992) can be realized in the following way: we vary the set of parameters $\Omega_m, \Omega_\Lambda, \Omega_\nu, \Omega_b, h, n_s$ and b_{cl} with fixed N_ν and find the minimum of χ^2 . Since N_ν can be discrete we repeat this procedure three times for $N_\nu=1, 2$, and 3. The lowest of the three minima is the minimum of χ^2 for the complete set of free parameters. Hence, we have seven free parameters. The formal number of observational points is 25 but, as we have mentioned, the 13 power spectra points can be described by just 3 degrees of freedom, so that the maximal number of truly independent measurements is 15. Therefore, the number of degrees of freedom for our search procedure is $N_F = N_{\text{exp}} - N_{\text{par}} = 8$ if all observational points are used. In order to investigate to what extent the LSS constraints on fundamental parameters match the constraints implied by SNIa (Perlmutter et al. 1999) we have determined all 8 parameters with and without the SNIa constraint (\hat{y}_{25}). The results are presented in the Table 1.

Note, that for all models χ^2_{min} is in the range $N_F - \sqrt{2N_F} \leq \chi^2_{\text{min}} \leq N_F + \sqrt{2N_F}$ which is expected for a Gaussian distribution of N_F degrees of freedom. This means that the cosmological paradigm which has been assumed is in agreement with the data. (Note here, that the reduction of the 13 not independent data points of the cluster power spectrum to three parameters is not important for our analysis since removing them from search procedure does not change the results essentially, as we will see later.)

Let us investigate how the parameters of the best fit model vary if we include also the data of the MAXIMA-1 experiment. The location and amplitude of the first acoustic peak determined from the combined Boomerang and MAXIMA-1 data are (Hu et al. 2000) $\ell_p = 206 \pm 6$, $A_p = 78.6 \pm 7$. If we use them instead values used above, the best fit parameters remain practically unchanged, $\Omega_m = 0.37 \pm 0.06$, $\Omega_\Lambda = 0.66 \pm 0.06$, $\Omega_\nu = 0.03 \pm 0.03$, $N_\nu = 1$, $\Omega_b = 0.039 \pm 0.010$, $n_s = 1.05 \pm 0.04$, and $h = 0.70 \pm 0.09$. Hence, including the MAXIMA-1 data into the determination of the first acoustic peak is not essential in our analysis and we will use here the values determined from the Boomerang data alone. This is however an important confirmation of the consistency of the two data sets.

We have also analyzed the influence of the amplitudes of the 2-nd and 3-d acoustic peaks on the determination of cosmological parameters in the frame of our approach. If we add to our data set their values and errors as determined by (Hu

et al. 2000) and calculate them using the analytical approximation given by the same authors then $\chi^2 \approx 18$, which is far too much for 9 degrees of freedom. In this case the best-fit parameters are $\Omega_m = 0.37 \pm 0.07$, $\Omega_\Lambda = 0.72 \pm 0.05$, $\Omega_\nu \approx 0$, $\Omega_b = 0.046 \pm 0.011$, $n_s = 0.97 \pm 0.03$, and $h = 0.67 \pm 0.08$. For the 2-nd acoustic peak and nucleosynthesis constraint the deviations of the predicted values from their observed counterparts are maximal (2.8σ higher, and 1.4σ higher respectively). If we exclude the nucleosynthesis constraint from the search procedure then $\chi^2/N_F \approx 7/8$ and best-fit parameters become $\Omega_m = 0.34 \pm 0.06$, $\Omega_\Lambda = 0.74 \pm 0.05$, $\Omega_\nu \approx 0$, $\Omega_b = 0.055 \pm 0.012$, $n_s = 0.98 \pm 0.03$, and $h = 0.72 \pm 0.08$. Practically all used constraints are satisfied but $\Omega_b h^2$ is 9σ higher than value deduced from the determination of the primeval deuterium abundance by (Burles et al. 1999) and 12σ higher than more recent value (Burles et al. 2000). This problem of the inconsistency of the Boomerang and MAXIMA-1 values for the height of the second peak especially with the nucleosynthesis constraint on the baryon abundance has been discussed at large in the recent literature (Lange et al. 2000; Tegmark & Zaldarriaga 2000b; Hu et al. 2000; Esposito et al. 2000; Durrer et al. 2000). Since we have nothing new to add to this subject here, we will not discuss it any further in this work. In what follows, we exclude the 2-nd and 3-d acoustic peaks from experimental data set in our search procedure but we will use them in the discussion of our best-fit model.

The errors in the best-fit parameters as presented in Table 1 are the square roots of the diagonal elements of the covariance matrix which is calculated according to the prescription given in Press et al. 1992 (Chaper 15) or Tegmark & Zaldarriaga 2000a (Appendix A).

4.2 The best-fit model

The model with one sort of massive neutrinos provides the best fit to the data, $\chi^2_{\text{min}} = 5.9$. However, there is only a marginal difference in χ^2_{min} for $N_\nu = 1, 2, 3$. With the given accuracy of the data we cannot conclude whether massive neutrinos are present at all and if yes what number of degrees of freedom is favored. We summarize, that the considered observational data on LSS of the Universe can be explained by a Λ MDM inflationary model with a scale invariant spectrum of scalar perturbations and a small positive curvature.

Including of the SNIa constraint into the experimental data set decreases Ω_m , increases Ω_Λ slightly and prefers $\Omega_\nu \approx 0$, a Λ CDM model.

In Table 2 we compare the values of the different observational constraints with the predictions for the best-fit models (Table 1 for $N_\nu = 1$). In both cases the calculated characteristics of the LSS are within the 1σ error bars of the observed values. In the last row we indicate the age of the Universe determined according to the general expression for non-zero curvature and non-zero Λ models (Sahni & Starobinsky 2000)

$$t_0 = H_0^{-1} \int_0^\infty \frac{dz}{\Omega_m(1+z)^5 + \Omega_k(1+z)^4 + \Omega_\Lambda(1+z)^2}. \quad (22)$$

The predicted age of the Universe agrees well with recent determinations of the age of globular clusters.

Comparing the results obtained without and with the

* We treat Ω_Λ and Ω_m as free parameters, $\Omega_k = 1 - \Omega_\Lambda - \Omega_m$.

Table 1. Cosmological parameters determined from the LSS data described in the text without and with the SNIa constraint. The errors indicated are the square roots of the diagonal elements of the covariance matrix.

N_ν	χ^2_{min}	Ω_m	Ω_Λ	Ω_ν	Ω_b	n_s	h
Without SNIa constraint							
1	5.90	0.37 ± 0.06	0.69 ± 0.07	0.03 ± 0.03	0.037 ± 0.009	1.02 ± 0.04	0.71 ± 0.09
2	6.02	0.42 ± 0.08	0.64 ± 0.09	0.04 ± 0.04	0.038 ± 0.010	1.03 ± 0.04	0.71 ± 0.09
3	6.17	0.47 ± 0.10	0.59 ± 0.08	0.06 ± 0.01	0.038 ± 0.010	1.04 ± 0.03	0.70 ± 0.09
Including SNIa constraint							
0-3	6.02	0.32 ± 0.05	0.75 ± 0.06	$< 10^{-4}$	0.038 ± 0.010	1.0 ± 0.05	0.70 ± 0.09

Table 2. Theoretical predictions for the used characteristics of the best-fit AMDM model with one sort of massive neutrinos with the cosmological parameters given in Table 1, first line (without SNIa constraint) and last line (including the SNIa constraint) are compared with observations.

Characteristics	Observations ^{a)}	Predictions	
		Without SNIa	Including SNIa
ℓ_p	197 ± 6	197	197
A_p	69 ± 8	71.5	71.9
V_{50} , km/s	375 ± 85	327	308
$\sigma_8 \Omega_m^{\alpha_1}$	0.60 ± 0.022	0.61	0.60
$\sigma_8 \Omega_m^{\alpha_2}$	0.56 ± 0.095	0.58	0.58
$\sigma_8 \Omega_m^{\alpha_3}$	0.8 ± 0.1	0.69	0.71
σ_F	$2.0 \pm .3$	1.9	1.9
$\Delta_\rho^2(k_p)$	0.57 ± 0.26	0.56	0.59
$n_p(k_p)$	-2.25 ± 0.2	-2.20	-2.20
h	0.65 ± 0.10	0.71	0.70
$\Omega_b h^2$	0.019 ± 0.0012	0.019	0.019
$\Omega_m - 0.75 \Omega_\Lambda$	-0.25 ± 0.125	-0.14	-0.25
t_0 , Gyrs ^{b)}	$13.2 \pm 3.0^c)$, $11.5 \pm 1.5^d)$	12.6	13.5

^{a)} all errors are $\pm 1\sigma$, ^{b)} is not used in the search procedure, ^{c)}(Carretta et al. 1999), ^{d)}(Chaboyer et al. 1998)

SNIa constraint, we conclude that the values of the fundamental cosmological parameters Ω_m , Ω_Λ and Ω_k determined by the observational characteristics of large scale structure match the SNIa test very well. This can be interpreted as independent support of the SNIa result in the framework of the standard cosmological paradigm. However, in order to elucidate how LSS data constraint cosmological parameters, we analyze further only the model obtained without the SNIa constraint.

The best fit values of cosmological parameters determined by LSS characteristics[†] are $\Omega_m = 0.37 \pm 0.06$, $\Omega_\Lambda = 0.69 \pm 0.07$, $\Omega_\nu = 0.03 \pm 0.03$, $N_\nu = 1$, $\Omega_b = 0.037 \pm 0.009$, $n_s = 1.02 \pm 0.04$, and $h = 0.71 \pm 0.09$. The CDM density parameter is $\Omega_{cdm} = 0.30 \pm 0.10$ and $\Omega_k = -0.06 \pm 0.13$. The neutrino content, which is compatible with zero is very

[†] We still include the direct measurement of h and the nucleosynthesis constraint in the analysis.

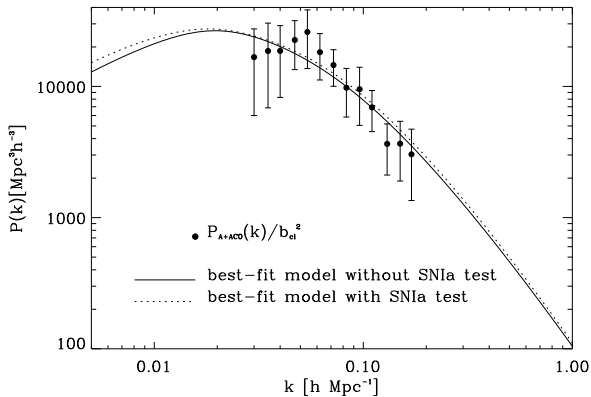
badly determined (100% error). The obtained value should be interpreted as an upper limit to the neutrino contribution. Below we will discuss this upper limit in more detail.

The value of the Hubble constant is close to the result by Madore et al. (1999) and Mould et al. (2000), somewhat higher than the directly measured value given in Eq. (8). The spectral index coincides with the prediction of the simplest inflationary scenario, it is close to unity. The neutrino matter density $\Omega_\nu = 0.03$ corresponds to a neutrino mass of $m_\nu = 94 \Omega_\nu h^2 \approx 1.4$ eV but is compatible with 0 within 1σ . The estimated cluster bias parameter $b_{cl} = 2.36 \pm 0.25$ fixes the amplitude of the Abell-ACO power spectrum (Fig. 1).

Recently, it has been shown (Novosyadlyj 1999) that due to the large error bars, the position of the peak of $\tilde{P}(k)$ at $k \approx 0.05h/\text{Mpc}$ does not influence the determination of cosmological parameters significantly. Only the slope of the power spectrum on scales smaller than the scale of the peak is relevant for cosmological parameters. On the other hand, the relation of the peak in $\tilde{P}_{A+ACO}(k)$ obtained from the

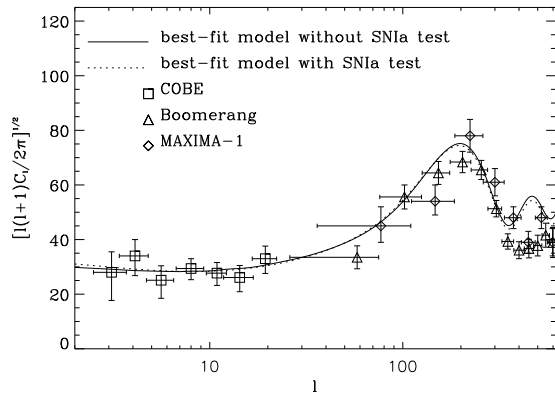
Table 3. Best-fit values of cosmological parameters determined from the different data set.

No	Data set	χ^2_{min}/N_F	Ω_m	Ω_Λ	Ω_ν	Ω_b	n_s	h
1	All observable data points are used	5.90/7	0.37	0.69	0.027	0.037	1.02	0.71
2	$\tilde{P}_{A+ACO}(k)$'s points are excluded	2.12/4	0.32	0.75	0.0	0.039	1.00	0.70
3	\tilde{l}_p, \tilde{A}_p are excluded	4.79/5	0.39	0.47	0.058	0.042	1.14	0.67
4	\tilde{V}_{50} is excluded	5.54/6	0.37	0.69	0.021	0.038	1.00	0.71
5	$\tilde{\sigma}_8 \Omega_m^{\alpha_1}$ is excluded	4.58/6	0.45	0.61	0.052	0.039	1.03	0.69
6	$\tilde{\sigma}_8 \Omega_m^{\alpha_2}$ is excluded	5.88/6	0.37	0.69	0.027	0.037	1.02	0.71
7	$\tilde{\sigma}_8 \Omega_m^{\alpha_3}$ is excluded	4.72/6	0.38	0.68	0.028	0.038	1.01	0.70
8	All $\tilde{\sigma}_8$ tests are excluded	3.85/4	0.49	0.57	0.060	0.041	1.04	0.68
9	the first Ly- α test is excluded	5.46/6	0.42	0.65	0.048	0.039	1.02	0.70
10	The second Ly- α test is excluded	5.81/5	0.37	0.69	0.026	0.037	1.02	0.71
11	Both Ly- α tests are excluded	4.49/4	0.56	0.50	0.21	0.042	1.04	0.67
12	The nucleosynthesis constraint is excluded	4.52/6	0.29	0.89	0.023	0.001	1.04	0.67
12	The direct constraint on h is excluded	4.18/6	0.29	0.71	0.038	0.023	1.05	0.91
13	Both previous constraints are excluded	4.16/5	0.29	0.71	0.041	0.013	1.07	0.87
14	$\tilde{V}_{50}, \tilde{\sigma}_8 \Omega_m^{\alpha_2}$ and $\Delta_\rho^2(k_p)$ are excluded	5.52/4	0.37	0.69	0.021	0.038	1.01	0.70
15	$\tilde{\sigma}_8 \Omega_m^{\alpha_2}$ and $\Delta_\rho^2(k_p)$ are excluded	5.88/5	0.37	0.68	0.028	0.037	1.02	0.71

**Figure 1.** The observed Abell-ACO power spectrum (filled circles) and the theoretical spectra predicted by closed Λ MDM models with parameters taken from Table 1 ($N_\nu = 1$).

space distribution of Abell - ACO clusters around us to the matter density of the power spectrum of entire Universe is still under discussion. Using numerical simulations, Retzlaff et al. (1997) have shown that the pronounced peak in the spectrum (the fifth data point in Fig. 1) could be purely due to cosmic variance. Therefore, it should not influence cosmological parameters. In fact, the maximum of our fitting curve is at a different position, which shows that this peak position is not relevant for the present work. The oscillation of the $\tilde{P}_{A+ACO}(k)$ around the best-fit $P(k)$ in Fig. 1 determined from all observable data on LSS reflects the real distribution of rich clusters of galaxies in the vicinity of $\sim 300h^{-1}\text{Mpc}$ of our own galaxy only. This is supported by similar features in spectra reconstructed from the expanded sample of Abell-ACO clusters (Miller & Batuski 2000) and IRAS Point Source Catalog Redshift Survey (Saunders et al. 2000; Hamilton et al. 2000).

Using CMBfast we have calculated the angular power

**Figure 2.** The CMB power spectra predicted by best-fit Λ MDM models with parameters from Table 1 ($N_\nu = 1$) and COBE DMR (Bennett et al. 1996), Boomerang (de Bernardis et al. 2000) and MAXIMA-1 (Hanany et al. 2000) experimental data.

spectra of CMB temperature fluctuations for both best-fit models. Comparison with the COBE, Boomerang and MAXIMA-1 experiments are shown in Fig. 2. The CMB power spectrum predicted by both best-fit models matches the data very well within the range of the first acoustic peak. But it does not reproduce the absence of a second peak inferred from the Boomerang and MAXIMA-1 data at $l > 350$. This problem has been discussed intensively in literature (Lange et al. 2000; Tegmark & Zaldarriaga 2000b; Hu et al. 2000; Esposito et al. 2000). The lack of power in this range strongly favors models with more baryons than compatible with standard cosmological nucleosynthesis. The MAXIMA-1 data reduces the problem somewhat but does not remove it entirely (Hu et al. 2000). However, as we shall discuss, the cosmological parameters which match Boomerang and MAXIMA-1 data at high spherical harmonics also strongly disagree with other LSS con-

straints used here (see Subsection 4.8 below). Furthermore, the Boomerang, MAXIMA-1 and other CMB data in this range do not match each other very well. This (and the amount of work already published on this subject some of which is cited above) prompted us to ignore the problem of the second peak in the CMB anisotropy spectrum in this work. Future flights of Boomerang and MAXIMA and/or the future projects MAP and Planck will certainly decide on this very important issue, but we consider it premature to draw very strong conclusions at this point.

Finally let us mention some global characteristics of a Universe with our best-fit cosmological parameters. Its age of $t_0 = 12.6$ Gyrs is in the range of values determined from the age of globular clusters (Chaboyer et al. 1998; Carretta et al. 1999). The deceleration parameter is $q_0 = -0.52$, in good agreement with the SNIa constraint presented above leading to (Perlmutter et al. 1998) $\tilde{q}_0 = -0.57 \pm 0.17$. The original deceleration ($q > 0$) changes into acceleration ($q < 0$) at the redshift $z_d \approx 0.55$. The 'equality epoch', $\rho_m(z_e) = \rho_\Lambda(z_e)$, corresponds to the redshift $z_e \approx 0.23$.

4.3 The influence of different experimental data

One important question is how sensitive our result responds to each data point. To estimate this, we exclude some data points from the search routine and re-determine the best-fit parameters. The results of this procedure are presented in Table 3. In all cases when data on the first acoustic peak are included $\Omega_m + \Omega_\Lambda \approx 1.06$, very slight positive curvature ($\Omega_k \approx -0.06$) but compatible with flat, i.e. the geometry is defined mainly by the position of the first acoustic peak. The LSS data without CMB measurements prefer an open Universe with $\Omega_k = 0.14$ (4 row in the Table 3). The value of Ω_m never exceeds 0.56, Ω_Λ is always larger 0.47 and in most cases $\Omega_\Lambda > \Omega_m$. The best-fit values of the spectral index n_s and h for the different observable data sets are in the relatively narrow ranges of, 0.99-1.14 and 0.67-0.72 respectively. The baryon content, Ω_b is fixed by the nucleosynthesis constraint. Without this constraint (12 row in Table 3) Ω_b is lower, $\Omega_b \approx 0.001$, even below the value inferred from the luminous matter in the Universe, $\Omega_{\text{lum}} \sim 7 \times 10^{-3}$.

The hot dark matter content, Ω_ν , is reduced mainly by the Ly- α constraints but it is poorly determined in all cases. If instead of or together with these Ly- α constraints we use those by McDonald et al. (2000) which reduce the power at small scales, then the best-fit value for the neutrino content is ≈ 0.07 . But in this case the predictions for Ly- α constraints by Gnedin (1998) and Croft et al. (1998) are out of their 1σ ranges. Moreover, the constraints by McDonald et al. (2000) are not in good agreement with other data, especially, Bahcall & Fan (1998) and the SNIa constraints. We have not included these constraints any further in our determination of cosmological parameters. Note however that the neutrino content is mainly constrained by the Ly- α data. If both Ly- α tests are excluded, the best fit value of Ω_ν raises to 0.21!

Excluding the direct measurement of the Hubble parameter from our search procedure leads to a substantially larger value of $h \sim 0.91$ which is in disagreement with the direct determination.

The comparison of the 1-st and 2-nd rows of Table 3 shows that the Abell-ACO power spectrum prefers a slope

Table 4. The best fit values of all the parameters with errors obtained by maximizing the (Gaussian) 68% confidence contours over all other parameters.

parameter	central value and errors	
	without SNIa constraint	with SNIa constraint
Ω_m	$0.37^{+0.25}_{-0.15}$	$0.32^{+0.20}_{-0.11}$
Ω_Λ	$0.69^{+0.15}_{-0.20}$	$0.75^{+0.10}_{-0.19}$
Ω_ν	$0.03^{+0.07}_{-0.03}$	$0.0^{+0.09}_{-0.0}$
Ω_b	$0.037^{+0.033}_{-0.018}$	$0.038^{+0.033}_{-0.019}$
n_s	$1.02^{+0.09}_{-0.10}$	$1.00^{+0.13}_{-0.10}$
h	$0.71^{+0.22}_{-0.19}$	$0.70^{+0.28}_{-0.18}$
b_{cl}	$2.4^{+0.7}_{-0.6}$	$2.2^{+0.8}_{-0.5}$

of the matter power spectrum in the range $0.02 \leq k \leq 0.1h/\text{Mpc}$ $n \sim -1.5$ which results in lowering Ω_Λ and introduces a small but non-zero neutrino content.

The constraints $\tilde{\sigma}_8 \Omega_m^{\alpha_2}$ (Viana & Liddle 1999) and $\Delta_\rho^2(k_p)$ have practically no influence on the determination of parameters (rows 6, 10 and 15) due to their large error bars. They can be removed from the data set which reduces the number of effective degrees of freedom to $N_F = 5$; this is important for the marginalization procedure.

4.4 Marginalization

The next important question is: which is the confidence limit for each parameter marginalized over the others. The straight forward answer is the integral of the likelihood function over the allowed range of all the other parameters. But for a 7-dimensional parameter space this is computationally time consuming. Therefore, we estimate the 1σ confidence limits for all parameters in the following way. By varying all parameter we determine the 6-dimensional χ^2 hyper-surface which contains 68.3% of the total probability distribution. We then project this hyper-surface onto each axis in parameter space. Its shadow on the parameter axes gives us the 1σ confidence limits for the cosmological parameter under consideration. The 1σ confidence limits obtained in this way for Λ MDM models with one sort of massive neutrinos are given in Table 4. Including $\tilde{\sigma}_8 \Omega_m^{\alpha_2}$ and $\tilde{\Delta}_\rho^2(k_p)$ does not change the marginalized limits significantly.

It must be noted that even though the upper 1σ edge for h is 0.93 when marginalized over all other parameters for the data used here, the resulting age of the Universe is still larger than the lowest value allowed for the age of the oldest globular clusters, $t_0 \approx 10$ Gyrs if $\Omega_\Lambda > 0.72$. In the Fig. 3 we present the constraints in the $\Omega_\Lambda - h$ plane given by the lower limit for the age of the Universe, 10 Gyrs, for models with zero- and positive curvature. The range above corresponding line is excluded by this limit. Thus, the lower limit for the age of the Universe additionally constrains the confidence limits on the parameters, h and Ω_k from above and on Ω_Λ from below.

We have repeated the marginalization procedure includ-

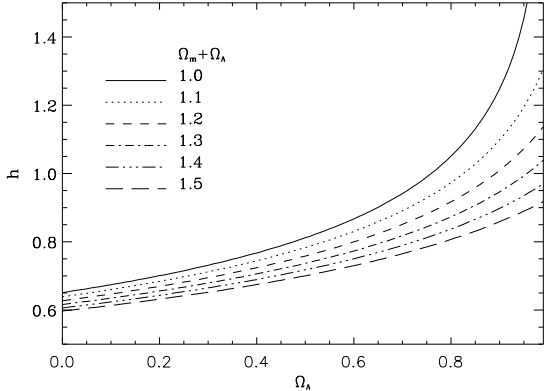


Figure 3. The lines in the $\Omega_\Lambda - h$ plane corresponding to the lower limit on age of the Universe of 10Gyrs established from oldest globular cluster for models with zero- and positive curvature. The range below the corresponding line is allowed.

ing the SNIa test (last column in Table 4). In this case we have to use all input data points (15 independent measurements), since neglecting $\hat{\sigma}_8 \Omega_m^{\alpha_2}$ and $\Delta_p^2(k_p)$ does somewhat change the marginalized limit. Hence, the number of degrees of freedom is $N_F = 8$ (1σ confidence limits corresponding to $\chi^2 \leq 15.3$). The SNIa test reduces the confidence ranges of Ω_m and Ω_Λ in spite of the larger number of degrees of freedom, but it results in somewhat wider 1σ error bars for the other parameters due to the increase of N_F and the low accuracy of the added data points.

4.5 The status of some subclasses of models

The errors shown in Table 4 define the range of each parameter within which by adjusting the remaining parameters a value of $\chi^2_{min} \leq 11.8$ can be achieved. Of course, the values of the remaining parameters always lay within their corresponding 68% likelihoods given in the Table 4. Models with vanishing Λ are outside of this marginalized 1σ range of the best-fit model determined by the LSS observational characteristics used here even without the SNIa constraint (column 2). Let us investigate the status of these models in more detail. For this, we set $\Omega_\Lambda = 0$ as fixed parameter and determine the remaining parameters in the usual way. The minimal value of χ^2 is $\chi^2 \approx 24$ with the following values for the other parameters: $\Omega_m = 1.15$, $\Omega_\nu = 0.22$, $N_\nu = 3$, $\Omega_b = 0.087$, $n_s = 0.95$, $h = 0.47$, $b_{cl} = 3.7$ ($\sigma_8 = 0.60$). This model is outside the 2σ confidence contour of the best-fit model for $N_\nu = 3$ (Table 1 without SNIa test). The experimental data which disagrees most with $\Lambda = 0$ is the data on the first acoustic peak. If we exclude it from the experimental data set, $\chi^2_{min} \approx 5.8$ for an open model with following best-fit parameters: $\Omega_m = 0.48$, $\Omega_\nu = 0.12$, $N_\nu = 1$, $\Omega_b = 0.047$, $n_s = 1.3$, $h = 0.64$, $b_{cl} = 2.5$ ($\sigma_8 = 0.82$). This model is inside the 1σ confidence contour of the best-fit ΛMDM model obtained without data on the first acoustic peak (row 3 of Table 3). The reason for this behavior is clear: the position of the ‘kink’ in the matter power spectrum at large scales demands a ‘shape parameter’ $\Gamma = \Omega_m h^2 \sim 0.25$ which can be achieved either by choosing an open model or allowing for a cosmological constant. The position of the

Table 5. The upper limits for the neutrino content and mass (in eV) at different confidence levels.

N_ν	Ω_ν	1σ C.L.		2σ C.L.		3σ C.L.	
		m_ν	Ω_ν	m_ν	Ω_ν	m_ν	Ω_ν
1	0.10	3.65	0.13	3.96	0.18	4.04	
2	0.15	2.79	0.21	3.06	0.29	3.35	
3	0.20	2.40	0.27	2.67	0.35	2.78	

acoustic peak which demands an approximately flat model then closes the first possibility.

Results change only slightly if instead of the Boomerang data we use Boomerang+MAXIMA-1 as discussed in Section 4.1. Hence, we can conclude that the LSS observational characteristics together with the Boomerang (+MAXIMA-1) data on the first acoustic peak already rule out zero- Λ models at more than 95% C.L. and actually demand a cosmological constant in the same bulk part as direct measurements. We consider this a non-trivial consistency check!

Flat Λ models in contrary, are inside the 1σ contour of our best-fit model. Actually, the best fit flat model has $\chi^2_{min} \approx 8.3$ and the best fit parameters $\Omega_m = 0.35 \pm 0.05$, $\Omega_\Lambda = 0.65 \pm 0.05$, $\Omega_\nu = 0.04 \pm 0.02$, $N_\nu = 1$, $\Omega_b = 0.029 \pm 0.005$, $n_s = 1.04 \pm 0.06$, $h = 0.81 \pm 0.06$, $b_{cl} = 2.2 \pm 0.2$ ($\sigma_8 = 0.96$) are close to our previous (Novosyadlyj et al. 2000a) results with a somewhat different observational data set.

It is obvious, that flat zero- Λ CDM and MDM models are ruled out by the present experimental data set at even higher confidence limit than by data without the Boomerang and MAXIMA-1 measurements in (Novosyadlyj et al. 2000a).

4.6 Upper limits for the neutrino mass

Since the neutrino content is compatible with zero, we determine an upper limit for it. We first determine the marginalized 1σ , 2σ and 3σ upper limits for Ω_ν for different values of N_ν . Using the best-fit value for h at given Ω_ν , we can then determine the corresponding upper limit for the neutrino mass, $m_\nu = 94 \Omega_\nu h^2 / N_\nu$. The results are presented in Table 5. For more species of massive neutrino the upper limit for Ω_ν is somewhat higher but m_ν is still lower for each C.L. The upper limit for Ω_ν raises with the confidence level as expected. But the upper limit for the mass grows only very little due to the reduction of the best-fit value for h . The upper limit for the combination $\Omega_\nu h^2 / N_\nu^{0.64}$ is approximately constant for all number species and confidence levels. The observational data set used here establishes an upper limit for the massive neutrino content of the universe which can be expressed in the form $\Omega_\nu h^2 / N_\nu^{0.64} \leq 0.042$ at 2σ confidence level. The corresponding upper limit on the neutrino mass $m_\nu \leq 4$ eV is close to the value obtained by (Croft et al. 1999).

4.7 Limiting the tensor mode

Up to this point we ignored uncertainties in the COBE normalization. The statistical uncertainty of the fit to the four-year COBE data, δ_h , is 7% (1σ) (Bunn and White 1997)

and we want to study how this uncertainty influences the accuracy of cosmological parameters which we determine.

Varying δ_h in the 1σ range we found that the best-fit values of all parameters except Ω_ν do not vary by more than 7% from the values presented in Table 1. Only Ω_ν , on which 1σ errors are of the order of 100%, varies in a range of 20%. These uncertainties are significantly smaller than the standard errors given in Table 1 and ignoring them is thus justified. (Including this error raises our standard 1σ errors from typically 10% - 20% to 11% - 21%).

Our results depend on a possible tensor component only via the COBE data which enters our calculation through the normalization constant δ_h , in Eqns. (11,12). We can estimate the maximal contribution of a tensor mode in the COBE $\Delta T/T$ data in the following way: we disregard the COBE normalization and consider δ_h as free parameter to be determined like the others. Its best-fit value then becomes $\delta_h^{LSS} = (2.95 \pm 2.55) \cdot 10^{-5}$ (for $N_\nu = 1$), while the best-fit values of the other parameters are $\Omega_m = 0.40 \pm 0.08$, $\Omega_\Lambda = 0.66 \pm 0.07$, $\Omega_\nu = 0.05 \pm 0.05$, $\Omega_b = 0.038 \pm 0.010$, $n_s = 1.14 \pm 0.31$, $h = 0.71 \pm 0.09$ and $b_{cl} = 2.4 \pm 0.3$. The best-fit value for density perturbation at horizon scale from the 4-year COBE data for this set of parameters is larger than the best-fit value determined from LSS characteristics, $\delta_h^{COBE} = 4.0 \cdot 10^{-5} > \delta_h^{LSS}$. This means that COBE $\Delta T/T$ data may contain a non-negligible tensor contribution. The most likely value of its fraction is given by $T/S = (\delta_h^{COBE} - \delta_h^{LSS})/\delta_h^{LSS}$. This value is $T/S = 0.36$ for the corresponding best-fit values of δ_h^{COBE} and δ_h^{LSS} from the Boomerang data alone and $T/S = 0.18$ from the combined Boomerang + MAXIMA-1 data. Since the standard error is rather large, $\approx 90\%$, we determine upper confidence limits for T/S by marginalizing δ_h^{LSS} over all the other parameters like we did for the neutrino content (see subsection 4.6). We then obtain $T/S < 1$ at 1σ C.L. and $T/S < 1.5$ at 2σ C.L. from the Boomerang data alone for the amplitude and position of the first acoustic peak. If we use the combined Boomerang + MAXIMA-1 data these limits are somewhat lower, 0.9 and 1.3 correspondingly, due to the higher amplitude of the first acoustic peak measured by MAXIMA-1. The 1σ upper constraint on the tensor mode obtained recently by Kinney et al. (2000) from the Boomerang and MAXIMA-1 data on the CMB power spectrum for the same class of models ($T/S < 0.8$ in our definition) is very close to the value obtained here.

4.8 Comparison with other parameter estimations

The cosmological parameters determined here from LSS+CMB data agree well with the values obtained by other methods (see e.g. the review by Primack (2000)). The marginalized 1σ ranges are still rather large due to the large experimental errors, the large number of parameters and the high degree of freedom. But this does, of course, not mean that an arbitrary set of parameters within the marginalized ranges matches the experimental data set with an accuracy $\leq 1\sigma$.

We compare our best fit model with others found in the recent literature by testing our data set as well as the Boomerang and MAXIMA-1 data on the CMB power spectrum. At first we calculate the predictions of the following models for our data set $(\Omega_m, \Omega_\Lambda, \Omega_b, n_s, h) = \mathbf{P} =$

(0.49, 0.56, 0.054, 0.92, 0.65) obtained by Lange et al. (2000) as best-fit model for the Boomerang and LSS data (denoted there as model P9); $\mathbf{P} = (0.68, 0.23, 0.07, 1, 0.6)$ obtained by Balbi et al. (2000) as best-fit model to the MAXIMA-1 and COBE DMR data; $\mathbf{P} = (0.35, 0.65, 0.036, 0.95, 0.8)$ obtained by Hu et al. (2000) as best-fit model to the Boomerang + MAXIMA-1 data on the first, second and third acoustic peaks; $\mathbf{P} = (0.3, 0.7, 0.045, 0.975, 0.82)$ obtained by Jaffe et al. (2000) as best-fit model to the Boomerang + MAXIMA-1 + COBE data on the CMB power spectrum; and the "concordance" model by Tegmark et al. (2000) which favors $\mathbf{P} = (0.38, 0.62, 0.043, 0.91, 0.63)$. Some authors give several sets of parameters obtained for different priors or by including different data sets, we take the one from which we obtain a minimal χ^2 for our data set. All these models have no massive neutrino component, no tensor mode and reionization is either not included or can be neglected. The predictions of cosmologies with the above parameters for the data considered in this work are presented in Table 6.

The χ^2 presented in last row includes also $\chi^2_{A+ACO} = \sum_{i=1}^{13} \left(\frac{P_{A+ACO}(k_i) - b_{cl}^2 P(k_i)}{\Delta P_{A+ACO}(k_i)} \right)^2$ which is small due to the cluster bias, b_{cl} , which is considered as free parameters in each model. In spite of the fact that all parameters of each model are within the marginalized 1σ ranges of the parameters of our best-fit model, the total value of χ^2 for the entire parameter sets rules out all the models at more than 2σ confidence level. Table 6 indicates the crucial tests. Models A and C are ruled out mainly by the nucleosynthesis constraint and the first σ_8 test (cluster mass function). Model B strongly disagrees with all σ_8 tests (14σ , 2.6σ and 1.6σ correspondingly), both Ly- α tests (2.6σ and 2.5σ), the nucleosynthesis constraint (5.2σ) and the data on the location of the first acoustic peak (5.6σ). Moreover, models A and B do not match the SNIa test which we have not included into χ^2 . Model D strongly disagree with nucleosynthesis constraint (9.4σ) and the Boomerang data on the location of the first acoustic peak (2.6σ). Model E does not match first and third σ_8 tests (at 5.1σ and 2.4σ respectively), the first Ly- α test (at 2.4σ) and the data on the location of the first acoustic peak (3.2σ). The latter is due to the fact that the MAXIMA-1 peak position is more than 1σ away from the peak position derived by the Boomerang data alone.

We now calculate the CMB power spectra for these models using CMBfast (version 3.2) and compare them with the experimental data from Boomerang (de Bernardis et al. 2000) and MAXIMA-1 (Hanany et al. 2000). The χ^2 deviations for all models including our best-fit model are presented in the Table 7. The first number indicates the χ^2 for the range of the first acoustic peak, $50 \leq \ell \leq 375$ (7 and 5 data points for the Boomerang and MAXIMA-1 experiments respectively), for the second number we have used the entire range, $50 \leq \ell \leq 750$ (12 and 10 data points for the Boomerang and MAXIMA-1 experiments respectively). In the range of the first acoustic peak our model fits as well as the other models, but the observed power spectrum at higher spherical harmonics is not reproduced by our model as we mentioned above.

Therefore, models which match the Boomerang and/or MAXIMA-1 CMB power spectrum at high spherical harmonics (in the range of second and third acoustic peak) disagree with some of the σ_8 , Ly- α and/or the nucleosynthesis

Table 6. Theoretical predictions for the observational values by best-fit models from the literature: A (Lange et al. 2000), B (Balbi et al. 2000), C (Hu et al. 2000), D (Jaffe et al. 2000), E (Tegmark et al. 2000).

Characteristics	Observations	Predictions				
		A	B	C	D	E
ℓ_p	197 \pm 6	206	231	206	213	225
A_p	69 \pm 8	57	68	63	72	62
V_{50} , km/s	375 \pm 85	280	310	303	293	239
$\sigma_8 \Omega_m^{\alpha_1}$	0.60 \pm 0.022	0.64	0.91	0.68	0.58	0.43
$\sigma_8 \Omega_m^{\alpha_2}$	0.56 \pm 0.095	0.62	0.93	0.65	0.65	0.42
$\sigma_8 \Omega_m^{\alpha_3}$	0.8 \pm 0.1	0.70	0.96	0.79	0.73	0.49
σ_F	2.0 \pm .3	1.7	2.8	2.2	1.9	1.1
$\Delta_p^2(k_p)$	0.57 \pm 0.26	0.51	1.21	0.81	0.62	0.25
$n_p(k_p)$	-2.25 \pm 0.2	-2.25	-2.15	-2.21	-2.22	-2.30
h	0.65 \pm 0.10	0.65	0.60	0.80	0.82	0.63
$\Omega_b h^2$	0.019 \pm 0.0012	0.023	0.025	0.023	0.030	0.02
$\Omega_m - 0.75\Omega_\Lambda$	-0.25 \pm 0.125	0.07	0.51	-0.13	-0.23	-0.09
χ^2		27	285	39	105	106

Table 7. The χ^2 deviation of theoretical predictions for the CMB power spectrum from experimental results for the models in Table 6 and for our best-fit model. The first number represents the the value of χ^2 for the CMB power spectrum in the range of the first acoustic peak, $50 \leq \ell \leq 375$, the second number is for the entire range $50 \leq \ell \leq 750$. Clearly our model parameters are in serious disagreement with the experimental CMB data beyond the first acoustic peak.

Experiment	χ^2					our best-fit model
	A	B	C	D	E	
Boomerang	7.3/12.6	77.2/96.7	6.1/12.8	18.3/24.5	13.6/24.5	11.3/108.5
MAXIMA-1	16.9/18.7	4.6/11.4	15.2/17.0	10.3/11.7	16.2/21.6	11.1/48.5

constraints. And vice versa, model which match very well the LSS observational characteristics predicts the CMB power spectrum which disagrees with measurements by Boomerang and MAXIMA-1 on very small scales. The resolution of this problem can go in several directions. If the Boomerang and MAXIMA-1 measurements are confirmed, nucleosynthesis may have been more complicated than assumed for the constraint used in this work (Esposito et al. 2000). An other problem may be the cluster mass function constraint which is exponentially sensitive to the value of σ_8 and might be too constraining, especially in view of all the uncertainties in the theory of cluster formation. Therefore, our constraint $\sigma_8 \Omega_m^{\alpha_1} = 0.60 \pm 0.022$ has to be taken with a grain of salt and its incompatibility with, e.g. the CMB data may also hint to a problem in the theory of cluster formation. Last but not least, if inconsistencies in the determination of cosmological parameters persist even after a serious improvement of data, e.g. with the Sloan digital sky survey, this may hint that the correct model is not within the class considered. If we want to fit a snail within the class of all known mammals by χ^2 minimization (or by a much more sophisticated method), we never obtain a very convincing fit.

5 CONCLUSIONS

The main observational characteristics on LSS together with recent data on the amplitude and location of the first acoustic peak in the CMB power spectrum, and the amplitude of the primordial power spectrum inferred by the COBE DMR four year data prefer a Λ MDM model with the following parameters: $\Omega_m = 0.37^{+0.25}_{-0.15}$, $\Omega_\Lambda = 0.69^{+0.15}_{-0.20}$, $\Omega_\nu = 0.03^{+0.07}_{-0.03}$, $N_\nu = 1$, $\Omega_b = 0.037^{+0.033}_{-0.018}$, $n_s = 1.02^{+0.09}_{-0.10}$, $h = 0.71^{+0.22}_{-0.19}$, $b_{cl} = 2.4^{+0.7}_{-0.7}$ (1σ marginalized ranges).

The central values correspond to a slightly closed ($\Omega_k = -0.06$) Λ MDM model with one sort of 1.4eV neutrinos. These neutrinos make up about 8% of the clustered matter, baryons are 10% and the rest (82%) is in a cold dark matter component. The energy density of clustered matter corresponds to only 35% of the total energy density of matter plus vacuum which amounts to $\Omega = 1.06$. The massive neutrino content is compatible with zero and we have established an upper limit in the form of $\Omega_\nu h^2 / N_\nu^{0.64} \leq 0.042$ at 2σ confidence level. The upper 2σ limit for the neutrino mass is 4.0eV.

If COBE normalization is disregarded, the best-fit value of the density perturbation at horizon scale is $\delta_h^{LSS} = (2.95 \pm 2.55) \cdot 10^{-5}$ while the best-fit values of the other parameters

are $\Omega_m = 0.40$, $\Omega_\Lambda = 0.66$, $\Omega_\nu = 0.05$, $N_\nu = 1$, $\Omega_b = 0.038$, $n_s = 1.14$, $h = 0.71$ and $b_{cl} = 2.4$. Comparison it with the best-fit value to the COBE 4-year data δ_h^{COBE} gives an estimate for the contribution of a tensor mode to the COBE DMR data: $T/S = 0.36^{+0.64}_{-0.36}$ from the Boomerang data on the first acoustic peak and $T/S = 0.18^{+0.72}_{-0.18}$ (1σ confidence limits) when the combined Boomerang+MAXIMA-1 data are used. The upper limits on T/S at 2σ C.L. for these two cases are 1.5 and 1.3 respectively.

The values for the matter density Ω_m and the cosmological constant Ω_Λ for the best-fit model are close to those deduced from the SNIa test. Including this test in the observational data set, results to a somewhat larger value of Ω_Λ (7%) and slightly lowers Ω_m .

The observational characteristics of large scale structure together with the Boomerang (+MAXIMA-1) data on the first acoustic peak rule out zero- Λ models at more than 2σ confidence limit.

ACKNOWLEDGMENTS

It is a pleasure to acknowledge stimulating discussions with Stepan Apuneyvych, Pedro Ferreira, Vladimir Lukash, Max Tegmark and Matts Roos. This work is part of a project supported by the Swiss National Science Foundation (grant NSF 7IP050163). B.N. is also grateful to Geneva University for hospitality.

REFERENCES

Bahcall, N.A., Fan, X., 1998, *ApJ*, 504, 1
 Balbi, A. et al. 2000, *astro-ph/0005124*
 Bennett, C.L. et al., 1996, *ApJ*, 464, L1
 Benson, A.J., et al., 2000, *MNRAS*, 314, 517
 Bertschinger, E., Dekel, A., Faber, S.M., Dressler, A. & Burstein, D., 1990, *ApJ*, 364, 370
 de Bernardis, P. et al., 2000, *Nature*, 404, 955
 Borgani, S. et al., 1999, *ApJ*, 527, 561
 Bridle, S.L., et al., 1999, *astro-ph/9903472*
 Bunn E.F., White M., 1997, *ApJ*, 480, 6
 Burles, S., Nollett, K.M., Truran, J.N., Turner, M.S., 1999, *Phys. Rev. Lett.*, 82, 4176
 Burles, S., Nollett, K.M. and Turner, M.S., 2000, *astro-ph/0010171*
 Carretta, E., Gratton, R.C., Clementini, G., Fusi Pecci, F., 1999, *ApJ* (in print), *astro-ph/9902086*
 Carroll, S.M., Press, W.H., Turner, E.L., 1992, *ARA&A*, 30, 499
 Chaboyer, B., Demarque, P., Kernan, P.J. and Krauss, L.M., 1998, *ApJ*, 494, 96
 Courteau, S., Faber, S.M., Dressler, A. & Willik, J.A., 1993, *ApJ*, 412, L51
 Croft, R.A.C. et al., 1998, *ApJ* 495, 44
 Croft, R.A.C., Hu, W., Dave, R., 1999, *Phys. Rev. Lett.*, 83, 1092
 Da Costa, L.N. et al., 1994, *ApJ*, 437, L1
 Dekel, A., 1994, *ARA&A*, 32, 371
 Dekel, A., 1999, *astro-ph/9911501*
 Durrer, R., Kunz, M. and Melchiorri, A., 2000 *astro-ph/0010633*
 Durrer, R. & Straumann, N., 1999, New methods for the determination of cosmological parameters. *Troisième Cycle de la Physique en Suisse Romande*, Université de Lausanne.
 Efstathiou, G. & Bond, J.R., 1999, *MNRAS*, 304, 75
 Einasto, J. et al., 1997, *Nature*, 385, 139
 Eisenstein, D.J., Hu, W., 1999, *ApJ*, 511, 5
 Esposito, S., Mangano, G., Melchiorri, A., Miele, G., Pisanti, O., 2000, *astro-ph/0007419*
 Fry, J. & Gaztañaga, E., 1993, *ApJ*, 413, 447
 Fukuda, Y. et al., 1998, *Phys. Rev. Lett.*, 81, 1562
 Girardi, M. et al., 1998, *ApJ*, 506, 45
 Gnedin N.Y., 1998, *MNRAS*, 299, 392
 Gnedin N.Y., 1999, private communication
 Hamilton, A. J. S., Tegmark, M. and Padmanabhan, N., 2000, *astro-ph/0004334*
 Hanany, S. et al., 2000, *astro-ph/0005123*
 Hu, W., Fukugita, M., Zaldarriaga, M. and Tegmark, M., 2000, *astro-ph/0006436*
 Jaffe, A.H. et al., 2000, *astro-ph/0007333*
 Kinney, W.H., Melchiorri, A., Riotto, A., 2000, *astro-ph/0007375*
 Kolatt, T., Dekel, A., 1997, *ApJ*, 479, 592
 Landy, S.D. et al., 1996, *ApJ*, 456, L1
 Lange, A.E. et al., 2000, *astro-ph/0005004*
 Liddle, A.R., Lyth, D.H., Viana, P.T.P., White, M., 1996, *MNRAS*, 282, 281
 Lineweaver, C.A., Barbosa, D., 1998, *ApJ*, 496, 624
 Lineweaver, C.A., 1998, *ApJ*, 505, L69
 Lyth, D.H. & Covi, L., 2000, *astro-ph/0002397*
 Maddox, S.J., Efstathiou, G., Sutherland, W.J., 1996, *MNRAS*, 283, 1227
 Madore, B.F. et al., 1999, *ApJ*, 515, 2941
 Melchiorri, A. et al., 2000, *ApJ*, 536, L63
 McDonald, P. et al., 2000, *ApJ*, 543, 1
 Miller, C. J. & Batuski, D. J., 2000, *astro-ph/0002295*
 Mould, J.R. et al., 2000, *ApJ*, 529, 786
 Novosyadlyj B., 1999, *Journal of Physical Studies*, 3, 122
 Novosyadlyj, B., Durrer, R., Gottloeber, S., Lukash, V.N., Apuneyvych, S., 2000, *A&A*, 356, 418 (*astro-ph/9912511*)
 Novosyadlyj, B., Durrer, R., Gottloeber, S., Lukash, V.N., Apuneyvych, S., 2000, *astro-ph/0002522*
 Park, C., Vogeley, M.C., Geller, M.J., Huchra, J.P., 1994, *ApJ*, 431, 569
 Perlmutter, S. et al., 1998, *Nature*, 391, 51
 Perlmutter, S. et al., 1999, *ApJ*, 517, 565
 Press, W.H., Flannery, B.P., Teukolsky, S.A., Vetrling, W.T., 1992, *Numerical recipes in FORTRAN*. New York: Cambridge Univ.Press
 Primack, J.R., 2000, *astro-ph/0007187*
 Primack, J.R. & Gross, M.A.K., 2000, *astro-ph/0007165*
 Retzlaff, J. et al., 1998, *New Astronomy*, 3, 631
 Ricotti, M., Gnedin, N.Y., Shull, J.M., 2000, *ApJ*, 534, 41 (*astro-ph/9906413*)
 Riess, A. et al., 1998, *AJ*, 116, 1009
 Sahni, V. & Starobinsky, A., 2000, *Int.J.Mod.Phys.*, D9, 373 (*astro-ph/9904398*)
 Saunders, W., Rowan-Robinson, M., Lawrence, A., 1992, *MNRAS*, 258, 134
 Saunders, W., Sutherland, W. J., Maddox, S. J. et al., 2000, *astro-ph/0001117*
 Seljak U., Zaldarriaga M., 1996, *ApJ*, 469, 437
 Tadros H., Estathiou G., 1996, *MNRAS*, 282, 1381
 Tadros H., Estathiou G. and Dalton, G., 1998, *MNRAS*, 296, 995
 Tammann, G.A., Federspiel, M., 1997, in "The Extragalactic Distance Scale", (eds.) M. Livio, M. Donahue, N. Panagia (Cambridge: Cambridge Univ. Press)
 Tegmark, M., 1999, *ApJ*, 514, L69
 Tegmark, M. & Zaldarriaga, M. 2000, *astro-ph/0002091*
 Tegmark, M. & Zaldarriaga, M., 2000, *astro-ph/0004393*
 Tegmark, M., Zaldarriaga, M. and Hamilton, A.J.S., 2000, *astro-ph/0008167*
 Viana, P.T.P. & Liddle, A.W., 1999, *MNRAS*, 303, 535
 Vogeley M., Park C., Geller M.J., Huchra J.P., 1992, *ApJ*, 391, L5